EVALUATION OF SPREAD SPECTRUM WATERMARKING SCHEMES IN THE WAVELET DOMAIN USING HVS CHARACTERISTICS

A. Zolghadrasli, Ph.D.
Department of Electronic Engineering
School of Engineering, Shiraz University
Shiraz, I. R. of Iran
Corresponding Author: zolghadr@shirazu.ac.ir

S. Rezazadeh, M.S.
Department of Electronic Engineering
School of Engineering, Shiraz University
Shiraz, I. R. of Iran

Abstract - In this paper, we introduce a multiresolution watermarking method for copyright protection of digital images. The method is based on the discrete wavelet transform. A noise type Gaussian sequence is used as watermark. To embed the watermark robustly and imperceptibly, watermark components are added to the significant coefficients of each selected subband by considering the human visual system (HVS) characteristics. Some small modifications are performed to improve the HVS model. The host image is needed in watermark extraction procedure, and Normalized Correlation Function (NCF) is used to measure similarities of extracted watermarks. It is shown that this method is robust against wide variety of attacks. Comparison with the existing methods shows the better performance of this suggested method.

Keywords - Watermarking, Non Oblivious Watermarking, Wavelet Transform, Spread Spectrum Watermarking, HVS Model.

INTRODUCTION

With the rapid growth of the Internet and the development of digital multimedia technologies, exchange and copy of digital multimedia have become quite convenient. Hence, the copyright protection of digital multimedia has become an important issue. A technique to solve this problem is digital watermarking, which embeds directly some digitized information into digital media by making small modifications to the media, where the watermark information remains detectable after attack. Thus, the digital watermarking can be used to identify the rightful owner.

Furthermore, it is an important issue to develope a robust watermarking scheme with a better tradeoff between robustness and imperceptibility [1]. Imperceptibility refers to the degree of distortion introduced by the watermark and its effect on the viewers or listeners. Robustness is the resistance of an embedded watermark against intentional attacks and normal A/V processes such as noise, filtering, resampling,

scaling, rotation, cropping, and lossy compression.

In image watermarking, two distinct approaches have been used to represent the watermark. In the first approach, the watermark is generally represented as a sequence of randomly generated real numbers having a normal distribution with zero mean and unity variance [2,3,4,5]. This type of watermark allows the detector to statistically check the presence or absence of the embedded watermark. In the second approach, a picture representing a company logo, or other copyright information, is embedded in the host image [6,7]. The detector actually reconstructs the watermark and computes its visual quality using an appropriate measure.

In recent years, watermarking has become an attractive topic and many watermarking schemes have been proposed. Among these schemes, the ones which require both the original information and secret keys for the watermarking extraction are called private watermark schemes. Schemes which require the watermark information and secret keys are called semi-private or semi-blind schemes. Schemes which need only secret keys without the original information are called public or blind watermark schemes [8].

Roughly speaking, digital watermarking schemes may be classified into two groups, spatial domain and transform domain watermarking. Spatial domain schemes embed messages in pixels of an image directly [9]. The least significant bit (LSB) scheme is the most common and the easiest method of this type. But the disadvantage is its lower security and susceptibility to distortion. For transform domain methods, images are transformed to frequency domain, and then messages are embedded into the frequency coefficients, such as DFT[1], DCT[2] and DWT[3]. Usually, the transform domain scheme is more robust against image processing attacks than spatial domain.

Due to the excellent time-frequency features and the well-matching to the human visual system (HVS) characteristics, wavelet has been widely used for digital watermarking, especially after the wavelet transform became the basic method in JPEG2000 standards several years ago. Many watermarking schemes have been proposed based on wavelet transform. In most wavelet domain watermarking schemes, watermark is embedded into the middle-frequency subbands coefficients, for two reasons: one is that low frequency components have more effects on the image quality than middle and high frequency components; the other is that high frequency components are easily removed after low pass filtering. In some schemes, the watermark is embedded into the DWT coefficients, where perceptual considerations are taken into account by setting the amount of modification proportional to the strength of the coefficient itself. Many other similar algorithms were then suggested by modifying Cox's scheme [2]. However, this kind of schemes generally does not consider human visual effects.

It is more reasonable to take the HVS model into account when embedding watermarks [10,11]. Authors in [11] have proposed a wavelet based multiresolution method using a human visual system, with the number of watermarks embedded proportional to the energy contained in each band. To enhance the invisibility of the watermarks, the characteristics of MTF[4] are used in their scheme. In this paper, we have proposed a watermarking method for embedding spread spectrum like watermarks in the wavelet domain. To embed the watermark robustly and imperceptibly, HVS characteristics are used in selecting the significant coefficients and adding the watermark to these coefficients. The HVS model we use here is based on the one that is proposed in [12] and improved in [13]. We have also performed small changes to this model to improve its performance for our watermarking method.

The rest of paper is organized as follows. First, we briefly review some basics on discrete wavelet transforms (DWT). The proposed algorithm for watermark embedding and extraction are explained after that. Later, the experimental results are presented. Finally, the concluding remarks are presented.

DISCRETE WAVELET TRANSFORM (DWT)

The wavelet transform has been extensively studied in the last decade. Many applications, such as compression, detection, and communications for wavelet transforms have been found [14,15].

The basic idea in the DWT for a one dimensional signal is the following: A signal is split into two parts, usually high frequency and low frequency components. The edge components of the signal are largely confined to the high frequency part. The low frequency part is split again into two parts of high and low frequencies. This process could be continued for an arbitrary number of times, the length of which is usually determined by the application at hand. Furthermore, from these DWT coefficients, the original signal can be reconstructed. This reconstruction process is called the inverse DWT (IDWT). The DWT and IDWT can be mathematically stated as follows:

Let

$$H(w) = \sum_k h_k e^{-jkw} \qquad \text{and} \qquad G(w) = \sum_k g_k e^{-jkw} \tag{1}$$

be a lowpass and a highpass filter, respectively, which satisfy a certain condition for reconstruction to be stated later. A signal, $x[n]$ can be decomposed recursively as:

$$c_{j-1,k} = \sum_n h_{n-2k} c_{j,n} \tag{2}$$

$$d_{j-1,k} = \sum_n g_{n-2k} c_{j,n} \tag{3}$$

For $j = J+1, J, \ldots, J_0$ where $c_{J+1,k} = x[k]$, $k \in \mathbf{Z}$, $J+1$ is the high resolution level index, and

J_0 is the low resolution level index. The coefficients: $c_{J_0,k}, d_{J_0,k}, d_{J_0+1,k}, \ldots, d_{J,k}$ are called the DWT of signal $x[n]$, where $c_{J_0,k}$ is the lowest resolution part of $x[n]$ and $d_{j,k}$ are the details of $x[n]$ at various bands of frequencies. Furthermore, the signal $x[n]$ can be reconstructed from its DWT coefficients, recursively.

$$c_{j,n} = \sum_k h_{n-2k} c_{j-1,k} + \sum_k g_{n-2k} d_{j-1,k} \tag{4}$$

The above reconstruction is called the IDWT of $x[n]$. To ensure the above IDWT and DWT relationship, the following orthogonality condition on the filters $H(w)$ and $G(w)$ is needed:

$$|H(w)|^2 + |G(w)|^2 = 1 \tag{5}$$

An example of such $H(w)$ and $G(w)$ is given by

$$H(w) = \frac{1}{2} + \frac{1}{2}e^{-jw} \quad \text{and} \quad G(w) = \frac{1}{2} - \frac{1}{2}e^{-jw}$$

which are known as the Haar wavelet filters.

The above DWT and IDWT for a one dimensional signal $x[n]$ can also be described in the form of two channel tree-structured filterbanks as shown in Figure 1. The DWT and IDWT for two dimensional images $x[m,n]$ can be similarly defined by implementing the one dimensional DWT and IDWT for each dimension m and n separately: $DWT_n[DWT_m[x[m,n]]]$, which is shown in Figure 2.

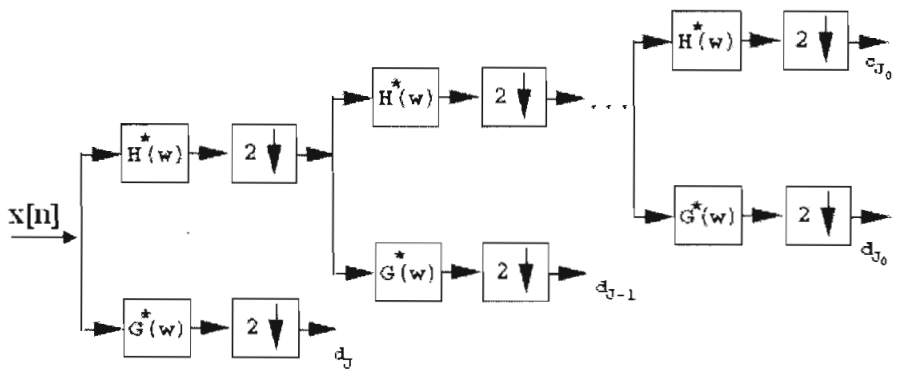

(a): DWT (decomposition).

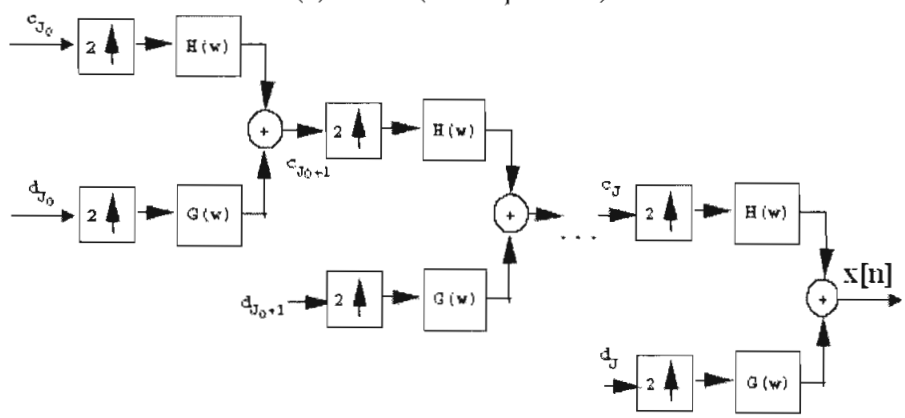

(b): IDWT (reconstruction).

Figure 1: DWT and IDWT for one dimensional signals.

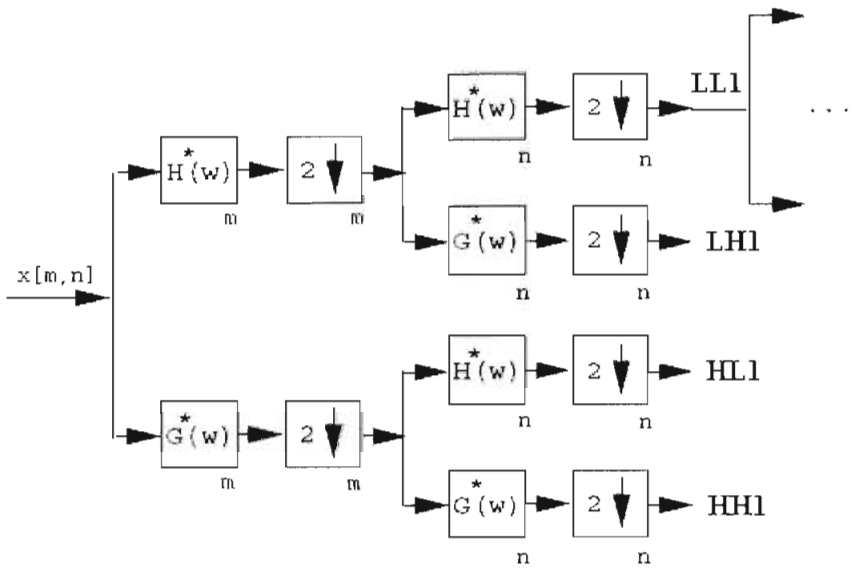

Figure 2: DWT for two dimensional images.

An image can be decomposed into a pyramid structure, shown in Figure 3, with various bands information: such as low-low frequency band (LL), low-high frequency band (LH), high-high frequency band (HH), etc. An example of such decomposition with two levels is shown in Figure 4, where the edges appear in all bands except in the lowest frequency band, i.e., the corner part at the left and top.

WATERMARKING METHOD

The proposed method embeds watermark by decomposing the host image using wavelet transforms. A visual mask based on HVS characteristics is used for calculating the weight factor for each wavelet coefficient of the host image and the significant coefficients from each subband are selected based on these weight factors.

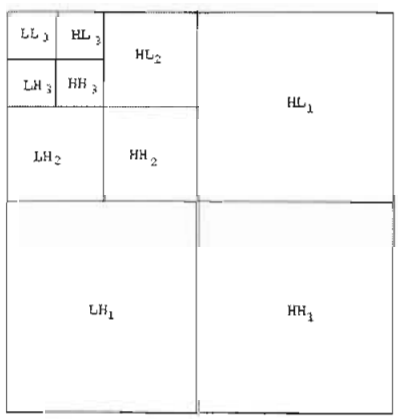

Figure 3: DWT pyramid decomposition of an image.

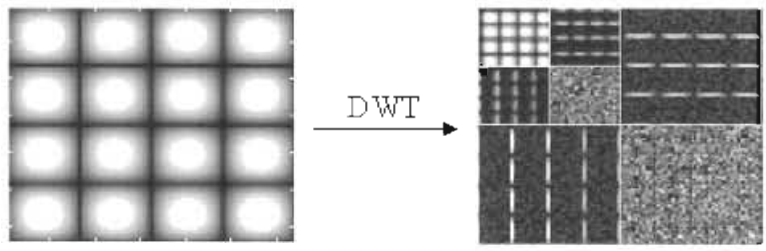

Figure 4: Examples of a DWT pyramid decomposition.

To embed the watermark in all selected wavelet coefficients, the watermark elements are added to the selected coefficients with their corresponding weight factors. These weight factors give the maximum amount of modification that can be applied to a wavelet coefficient without any perceptual degradation.

We represent the host image and watermark with I and W respectively. The host image is a grayscale image and the embedded watermark is a sequence of real numbers with Gaussian distribution such that:

$$W=\{w_1, w_2,\ldots, w_N\}$$

Where each element w in W is drawn independantly according to $N(0,1)$ (Normal distribution with mean=0 and variance=1). The main ideas of our method are explained in the following sections:

- HVS MODEL

Here, we use the human visual system which is introduced in [12,13] with some modifications to improve it. This model takes into account a number of factors like luminance, frequency band, texture and proximity to an edge. These factors are based on the following observations. Human eye is less sensitive to the areas of an image where brightness is high or low. Human eye is less sensitive to noise in high frequency subbands and bands having orientations of ±45°. Sensitivity of human eye to noise in textured area is less and near the edges is more.

To describe better the model, the wavelet representation of 4-levels transformed image is shown in Figure 5. Each subband is represented with $I_l^{\theta}(i,j)$ where $\theta \in \{0,1,2,3\}$ is the orientation and $l \in \{0,1,2,3\}$ gives resolution level of image. The weighting function $S_l^{\theta}(i,j)$ can be computed as product of three terms:

$$S_l^{\theta}(i,j) = \Theta(l,\theta)\cdot\Lambda(l,i,j)\cdot\Xi(l,i,j)^{0.2} \quad (6)$$

where the above three terms represent the sensitivity to noise changes in the bands, the local brightness and the local texture activities, respectively.

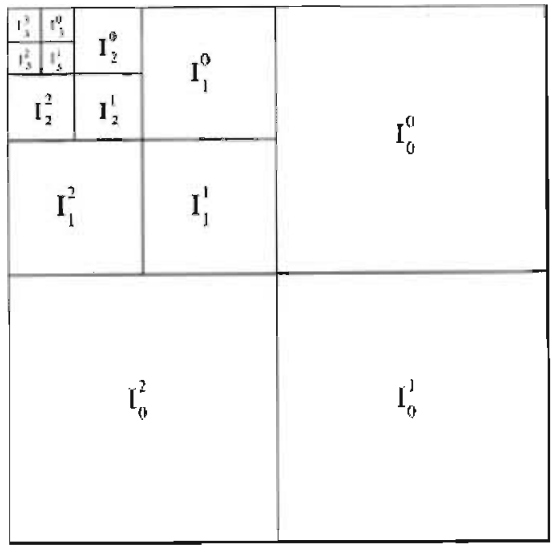

Figure 5: The 4-level DWT representation.

Depending on the orientation and resolution level, the first term, $\Theta(l,\theta)$ is computed in a similar way to that of [13] as follows:

$$\Theta(l,\theta)=\begin{Bmatrix}\sqrt{2} & if\ \theta=1\\ 1 & otherwise\end{Bmatrix}\cdot\begin{Bmatrix}1.00 & if\ l=0\\ 0.32 & if\ l=1\\ 0.16 & if\ l=2\\ 0.10 & if\ l=3\end{Bmatrix} \tag{7}$$

In [13], the second term $\Lambda(l,\ i,\ j)$, is computed using the coarsest approximation subband, $I_3^3(i,j)$ for evaluating the local brightness at all the resolution levels. However, this coarsest approximation band at the top-left corner is usually too small to contain enough information. In fact, to assess accurately the local brightness at a given resolution level, the reconstructed approximation subband at that level is a better choice. Therefore, we compute the second term in a new way as:

$$\Lambda(l,i,j)=1+L'(l,i,j) \tag{8}$$

where

$$L'(l,i,j)=\begin{cases}1-I_l^3(i,j) & if\ \ I_l^3(i,j)<0.5\\ I_l^3(i,j) & Otherwise\end{cases} \tag{9}$$

Finally, based on the above consideration, the third term, which measures the texture activity in the neighborhood of a coefficient, is computed in a different way to that in [13] as the following:

$$\Xi(l,i,j)=\sum_{k=0}^{3-l}\frac{1}{16^k}\sum_{\theta=0}^{2}\sum_{x=-1}^{1}\sum_{y=-1}^{1}\left[I_{k+l}^{\theta}\left(y+\frac{i}{2^k},x+\frac{j}{2^k}\right)\right]^2\cdot Var\left\{I_l^3(i,j)\right\} \tag{10}$$

Both these contributions are computed in a small 3×3 neighborhood corresponding to the location $(i,\ j)$ of the pixel. The first contribution can represent the distance from the edges, whereas the second one is the local variance of the corresponding

reconstructed approximation subband in a small neighborhood and measures the texture.

- WATERMARK EMBEDDING AND EXTRACTION

The algorithm for embedding is formulated as follows:

Step 1- Decompose host image up to 4-levels using DWT.

Step 2- Find out the weight factors $S_l^{\theta}(i,j)$ for wavelet coefficients using the weighting function in the previous section.

Step 3- Weight factors of each subband are sorted in descending order and then significant coefficients in each band are found out based on their weight factors.

Step 4- Add watermark sequence to the B percent ($25< B <75$) of significant coefficients in each subband (excluding $I_3^3(i,j)$) with the following formula:

$$I_l^{\theta,w}(i,j)=I_l^{\theta}(i,j)+\alpha S_l^{\theta}(i,j)w_k \quad , \ 1\le k\le N \tag{11}$$

where α is a global parameter accounting for watermark strength and N is the length of watermark.

Step 5- After embedding watermark sequence, the 4-level inverse wavelet transform of the watermarked coefficients is found out to give the watermarked image I_w.

For watermark extraction from watermarked image, the original unwatermarked image is also needed. In watermark extraction, a possibly distorted watermark W^* is extracted from the possibly distorted watermarked image A_w^* by reversing essentially the above watermark embedding steps. After watermark extraction, we compare the extracted watermark W^* with original watermark W by calculating their normalized correlation factor $NCF(W,W^*)$ with the following equation:

$$NCF(W,W^*)=\frac{\sum_{i=1}^{N}W(i)\times W^*(i)}{\sqrt{(\sum_{i=1}^{N}W^2(i))\times(\sum_{i=1}^{N}W^{*2}(i))}} \tag{12}$$

The normalized correlation is then compared with a threshold T to decide if the watermarks match or not. If $NCF\ge T$, then we say a watermak exists in the image. The threshold T can be determined by calculating false positive probability function (P_{FP}) according to the equation:

$$P_{FP}=\frac{\int_0^{\cos^{-1}(T)}Sin^{N-2}(u)\,du}{2\int_0^{\pi/2}Sin^{N-2}(u)\,du} \tag{13}$$

where N is the length of the watermark [16].

EXPERIMENTAL RESULTS

To test the performance of the proposed method, we choose 3 different grayscale

images with size of 512×512 pixels as host images. Figure 6 shows the host images. A Gaussian random noise with the size of 128×128 is used for watermark embedding. We determine the threshold T using Equation 13. To calculate the threshold, we set the P_{FP} to a very small value for example 10^{-9} and then T is computed. The value of threshold is 0.04, which is fixed during all experiments. For 4-level wavelet decomposition, "Daubechies 1" filter coefficients are used. This filter wavelet is selected because of its simplicity and linear phase. In watermark embedding, B is 50 and α is chosen such that the PSNR of watermarked images be 38 dB in all cases. PSNR is calculated using formula (14). This value of PSNR is chosen to have good tradeoff between robustness and imperceptibility.

$$PSNR(I, I_W) = 10 \log_{10} \left[\frac{\max_{\forall(x,y)} I^2(x,y)}{\frac{1}{N_I} \Sigma_{\forall(x,y)} (I_W(x,y) - I(x,y))^2} \right] \quad (14)$$

where N_I is the number of pixels in I. Watermarked images and their amplified differences with their originals are shown in Figure 7 and Figure 8 respectively. It can be observed form Figure 8 that the most part of the watermark sequence is stored in high textured regions where HVS is less sensitive.

(a) (b) (c)

Figure 6: Host images (a) Plane (b) Barbara (c) Baboon.

(a) (b) (c)

Figure 7: Watermarked images (a) Plane (b) Barbara (c) Baboon.

(a) (b) (c)

Figure 8: Amplified difference images (a) Plane (b) Barbara (c) Baboon.

Robustness of the proposed method is evaluated under various types of image distortions like adding noise, low-pass filtering, JPEG compression, image cropping, scaling and histogram equalization. In order to put the performance investigation of the algorithm in proper context, we compare our method with three other methods. These methods are Cox[2], Xia[3], Zhu[4].

Figures 9 to 11 show the results of adding Gaussian noise. We first obtain the watermarked image according to (11) and then add Gaussian noise to it. The mean of the additive Gaussian white noise is zero and its variance can change. By performing the watermark detection, we obtain the corrupted watermark W^*. Then, the normalized correlation factor between W (original watermark) and W^* is computed. Higher Normalized Correlation value means more robustness.

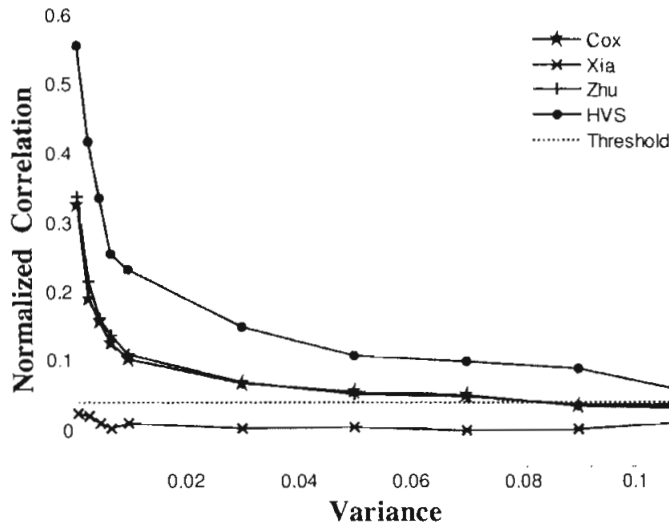

Figure 9: Robustness test against adding noise for image Plane.

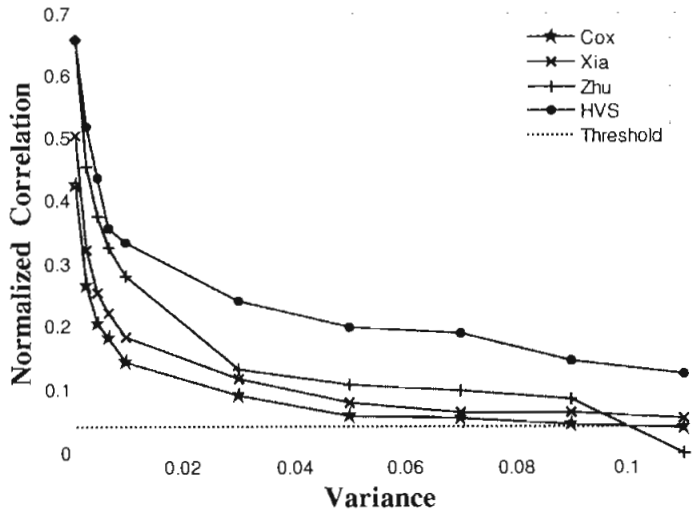

Figure 10: Robustness test against adding noise for image Barbara.

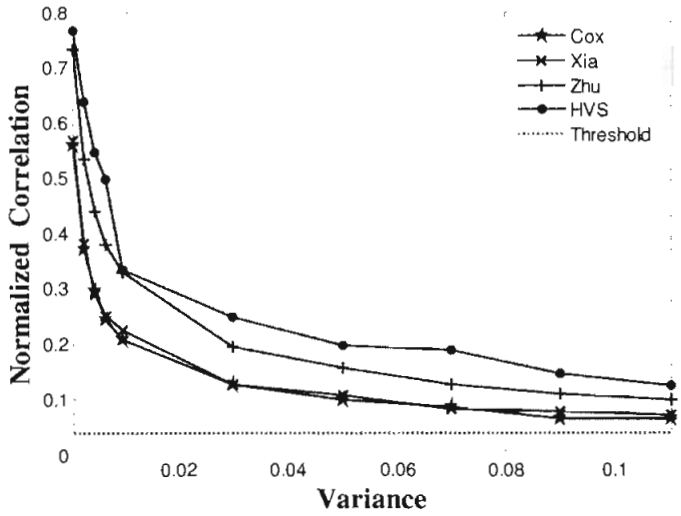

Figure 11: Robustness test against adding noise for image Baboon.

Figures 12 to 14 show the results of detecting the watermark with the proposed method on low-pass filtered images. The filter is a Gaussian low-pass filter. Its size is 20×20 and the variance is variable. We use the filter to perform a 2-D FIR filtering on the watermarked image. After filtering, the image becomes considerably smooth. We observe that after this process, our proposed algorithm can still reliably detect the correct watermark.

We also perform lossy compression for the watermarked images. Figures 15 to 17 show the robustness test against JPEG compression for different methods. We apply heavy compression to the watermarked images for different quality factors and then perform correlation detection. We can see that, even after heavy compression (compression ratio=47), the watermark can be well detected. The figures indicate that our method is robust against image compression.

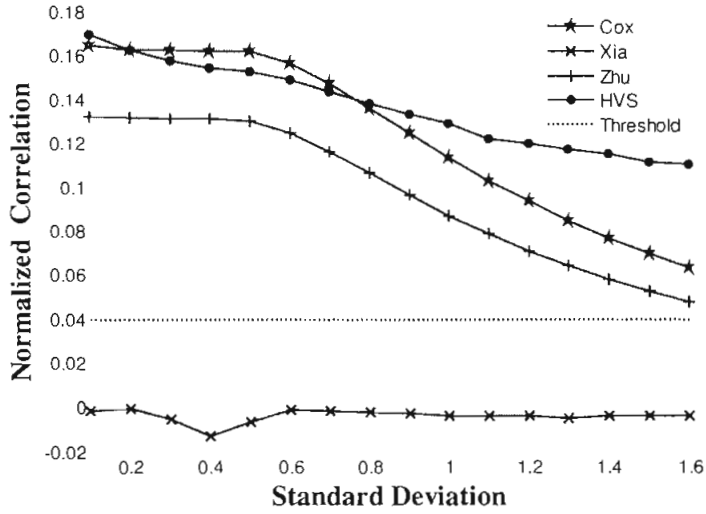

Figure 12: Robustness test against low-pass filtering for image Plane.

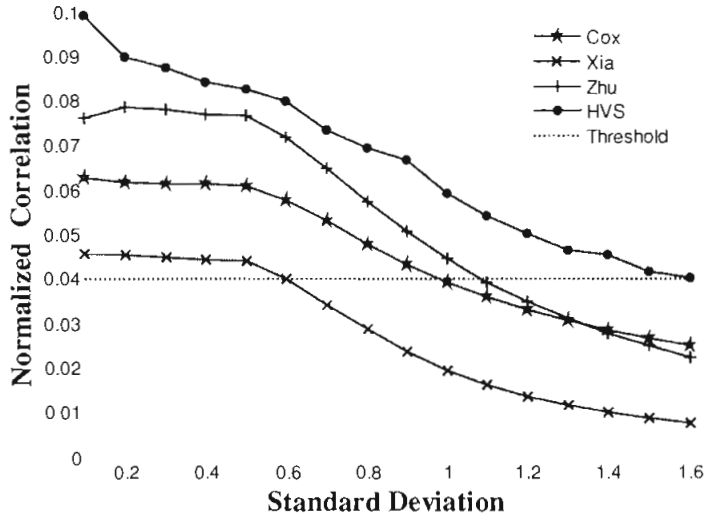

Figure 13: Robustness test against low-pass filtering for image Barbara.

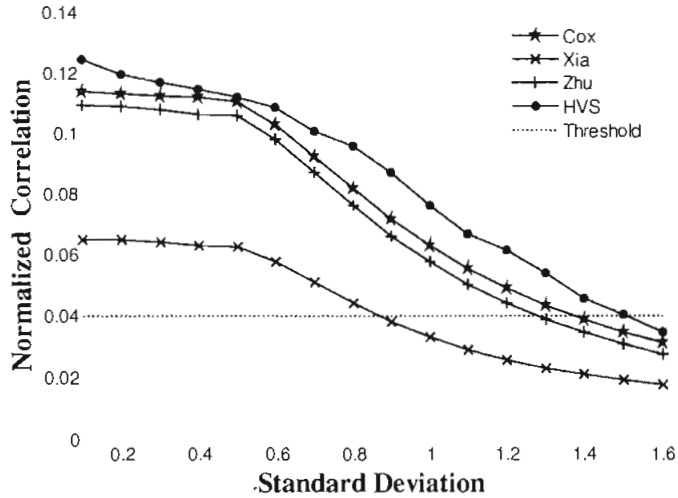

Figure 14: Robustness test against low-pass filtering for image Baboon.

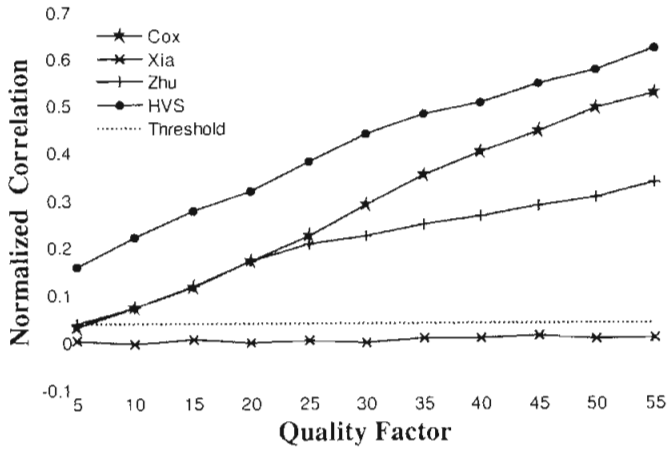

Figure 15: Robustness test against JPEG compression for image Plane.

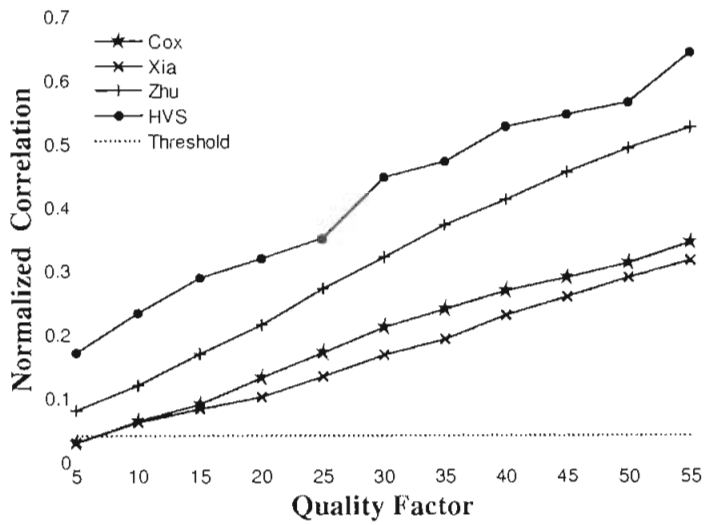

Figure 16: Robustness test against JPEG compression for image Barbara.

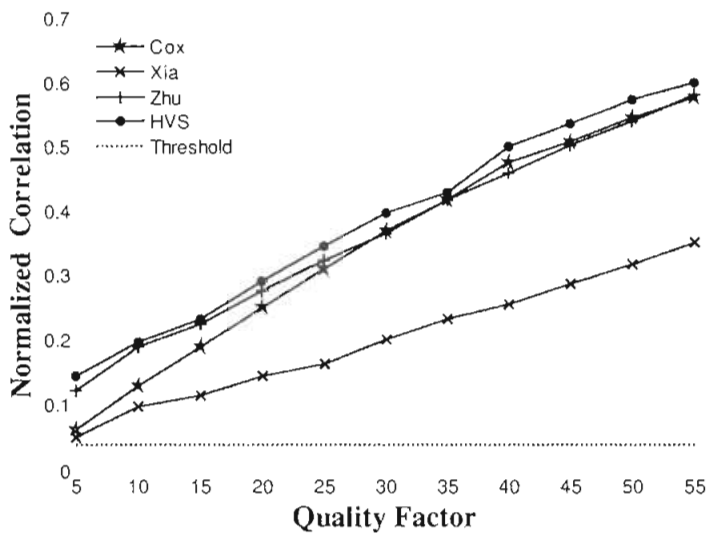

Figure 17: Robustness test against JPEG compression for image Baboon.

Figures 18 to 20 show the test for robustness against image cropping. First, we crop the watermarked image from its center with different dimensions and then detect existence of the watermark from the remaining data.

We have checked the robustness test against image re-sizing and histogram equalization too. Responses of correlation detection of given watermark under these two cases are given in Tables 1 and 2. In image resizing, we scaled the watermarked image to half of its original size at first. In order to recover the watermark, the quarter-sized image was rescaled to its original dimensions using bicubic interpolation. It can be seen from these tables that watermark can be detected properly under these two attacks.

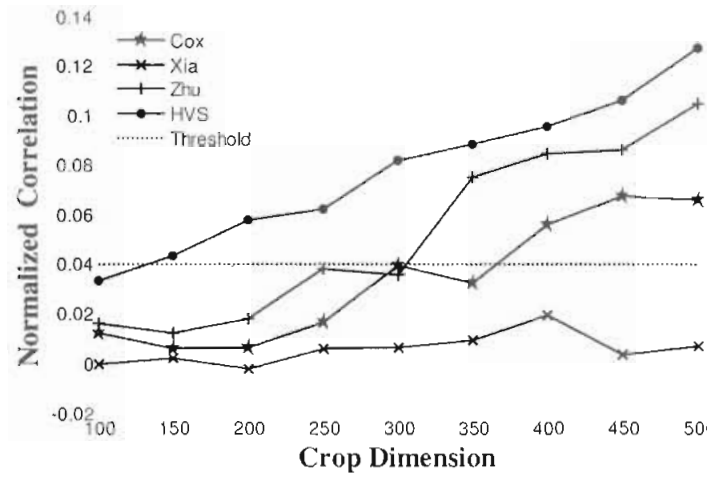

Figure 18: Robustness test against image cropping for image Plane.

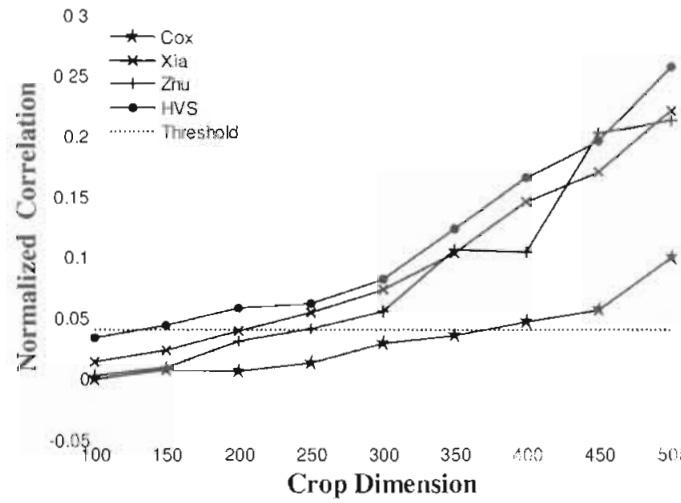

Figure 19: Robustness test against image cropping for image Barbara.

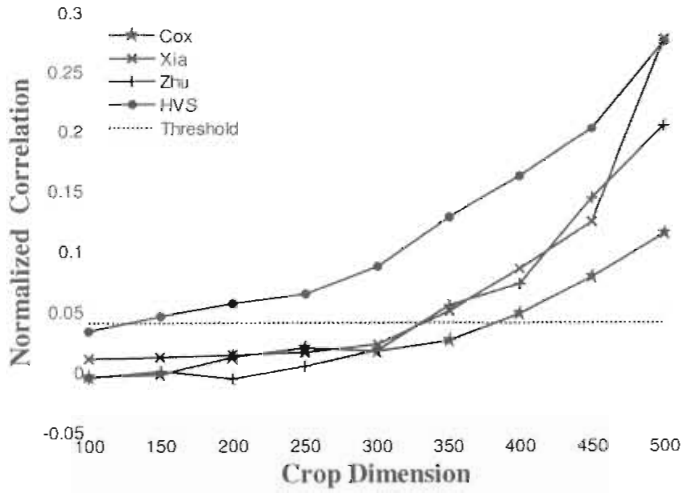

Figure 20: Robustness test against image cropping for image Baboon.

Table 1: Robustness test against image resizing.

	Plane	Barbara	Baboon
Cox	0.2852	0.0486	0.1030
Xia	0.0028	0.0301	0.0472
Zhu	0.1956	0.0650	0.0930
HVS	0.2245	0.0911	0.1189

Table 2: Robustness test against histogram equalization.

	Plane	Barbara	Baboon
Cox	0.2533	0.1675	0.1691
Xia	0.0148	0.2452	0.1747
Zhu	0.1864	0.2881	0.2390
HVS	0.1925	0.2901	0.2411

CONCLUSIONS

In this paper, we introduced a multiresolution watermarking method using the discrete wavelet transform. In this method, Gaussian random noise is added to the coefficients based on the selected weight factors calculated using the HVS characteristics. Normalized correlation function is used in watermark detection and threshold determination. Robustness of the algorithm is tested against different types of attacks. Finally, to show the superiority of this method we compared our results with the results of some other well-known methods. From the results it is observed that this method shows better robustness to attacks than other methods.

ACKNOWLEDGEMENT

This research is sponsored by ITRC (Iran Telecommunication Research Center) Tehran, Iran.

ENDNOTES

1. Discrete Fourier Transform
2. Discrete Cosine Transform
3. Discrete Wavelet Transform
4. Modulation Transfer Function

REFERENCES

[1] Barni, M., et al., "Improved Wavelet-Based Watermarking Through Pixel-Wise Masking." *IEEE Transactions on Image Processing*, Vol. 10, No. 5, pp. 783-791, 2001.

[2] Celik, M. U., et al., "Lossless Generalized-LSB Data Embedding." *IEEE Transactions on Image Processing*, Vol. 14, No. 2, pp. 253-266, 2005.

[3] Choi, Y. H. and Choi, T. S., "Robust Logo Embedding Technique for Copyright Protection." *IEEE International Conference on Consumer Electronics*, pp. 341-342, 2005.

[4] Cox, I. J., et al., "Secure Spread Spectrum Watermarking for Multimedia." *IEEE Transactions on Image Processing*, Vol. 6, No. 12, pp. 1673-1687, 1997.

[5] Cox, I. J., et al., *Digital Watermarking*. San Francisco, Morgan Kaufmann Inc, 2002.

[6] Jansen, M. and Oonincx, P., *Second Generation Wavelets and their Applications*. Springer Verlag, New York, 2005.

[7] Kim, Y. S., et al., "Wavelet Based Watermarking Method for Digital Images Using the Human Visual System." *Electronics Letters*, Vol. 35, No. 6, pp. 466-468, 1999.

[8] Kundur, D. and Hatzinakos, D., "Toward Robust Logo Watermarking Using Multiresolution Image Fusion Principles." *IEEE Transactions on Multimedia*, Vol. 6, No. 1, pp. 185-198, 2004.

[9] Langelaar, G. C., et al., "Watermarking Digital Image and Video Data: A State-of-the-Art Overview." *IEEE Signal Processing Magazine*, Vol. 17, No. 5, pp. 20-46, 2000.

[10] Lewis, A. S. and Knowles, G., "Image Compression Using the 2-D Wavelet Transform." *IEEE Transactions on Image Processing*, Vol. 1, pp. 244-250, 1992.

[11] Maity, S. P. and Kundu, M. K., "An Image Watermarking Scheme Using HVS Characteristics and Spread Transform." *IEEE International Conference on Pattern Recognition*, Vol. 4, pp. 869-871, 2004.

[12] Nikolaidis, A. and Pitas, I., "Asymptotically Optimal Detection for Additive Watermarking in the DCT and DWT Domains." *IEEE Transactions on Image Processing*, Vol. 12, No. 5, pp. 563-571, 2003.

[13] Walnut, D. F., *An Introduction to Wavelet Analysis*. Boston, Birkhauser Inc, 2002.

[14] Wong, P. H. W., et al., "A Novel Blind Multiple Watermarking Technique for Images." *IEEE Transactions on Circuits and Systems for Video Technology*, Vol. 13, No. 8, pp. 813-830, 2003.

[15] Xia, X. G., et al., "Wavelet Transform Based Watermark for Digital Images." *Optics Express*, Vol. 3, No. 12, pp. 497-511, 1998.

[16] Zhu, W., et al., "Multiresolution Watermarking for Images and Video." *IEEE Transactions on Circuits and Systems for Video Technology*, Vol. 9, No. 4, pp. 545-550, 1999.